Self-diffusion in tungsten

J. N. Mundy, S. J. Rothman, N. Q. Lam, H. A. Hoff, and L. J. Nowicki
Materials Science Division, Argonne National Laboratory, Argonne, Illinois 60439
(Received 6 June 1978)

Self-diffusion in tungsten single crystals has been measured over the temperature range 1700–3400 K (encompassing a range of nine orders of magnitude in the diffusion coefficient D). The plot of $\ln D$ vs $1/T$ is curved, and can be fitted by a sum of two exponentials, $D = 0.04\exp(-5.4_5 eV/kT) + 46\exp(-6.9\times eV/kT)$ cm^{2}sec^{-1}, the first of which probably represents diffusion by single vacancies.

I. INTRODUCTION

Precise measurements of self-diffusion in metals over a wide temperature range have been helpful in the elucidation of parameters for point-defect motion and formation. Measurements on the face-centered-cubic (fcc) metals Ag,[1-4] Cu,[5-8] Au,[9-13] and Ni,[14,15] have shown a gentle upward curvature of the Arrhenius plot of $\ln D$ vs $1/T$, where D is the diffusion coefficient; this has been interpreted in terms of simultaneous diffusion by vacancies and divacancies[16,17] or temperature-dependent diffusion parameters.[18] Fairly precise estimates of the activation energy for diffusion by single vacancies Q_{1v}^{self} and rather less-precise estimates of Q_{2v}^{self}, have been obtained from the diffusion data for these metals. There is usually good consistency between the values of Q_{1v}^{self} obtained from measurements of self-diffusion and the single-vacancy parameters obtained from other types of experiments, such as quenching and annealing studies and positron annihilation.[19,20] Thus the relation of point-defect behavior to diffusion in fcc metals is fairly well understood, although areas of controversy still remain.

In some body-centered-cubic (bcc) metals, self-diffusion can be measured only over the narrow temperature range in which the bcc phase is stable.[21] Among the bcc metals in which self-diffusion has been measured over a wide range of temperatures, the group IV-B metals Ti (Ref. 22) and Zr (Ref. 23) show much more strongly curved Arrhenius plots than the fcc metals, and are referred to as "anomalous diffusers."[21-24] On the other hand, the group V-B metals V,[25-27] Nb,[28] and Ta,[29] as well as the alkali metals Na,[30] and K,[31] show curvatures in their Arrhenius plots for self-diffusion that are similar to those of the fcc metals. Their diffusion behavior can again be interpreted in terms of diffusion via single vacancies and divacancies with $Q_{2v}^{self}/Q_{1v}^{self}\approx 1.28$, but the contribution from divacancies at the melting point T_m is an order of magnitude larger than that found for fcc metals.

Of the group VI-B metals, measurements on molybdenum[32,33] have been made over temperature spans that are too narrow to detect curvature. Chromium displays a straight Arrhenius plot over a range of almost six orders of magnitude in D values, but with a preexponential factor and activation energy so high as to suggest diffusion by divacancies alone.[34] The data available on tungsten[35-41] at the time the present work was begun were rather scattered, with no single investigation extending over a wide enough range of temperatures to reveal curvature (Fig. 1). Part of the scatter in the data was due to inadequacies in experimental technique, as pointed out by Arkhipova *et al.*, whose careful measurements[42] appeared while the present work was in progress. Polycrystalline samples were used in some of the low-temperature studies,[35,37,40,41] and the results from these studies may have been affected by grain-boundary diffusion. The results obtained by Pawel and Lundy[39] and Arkhipova *et al.*[42] on single crystals, and the results of Andelin and Knight,[36] appear to be the most reliable to date, but none of these studies extends over a wide range of temperatures.

On the other hand, tungsten appears to have excellent potential for use in determination of the point-defect parameters for a bcc transition metal; it is less susceptible to contamination by interstitial impurities than the group V-B elements, and its vacancy parameters have been studied by quenching[43,44] and by positron annihilation.[45] These considerations suggested that a new set of measurements of self-diffusion in tungsten, carried out on single crystals over a wide temperature range, would be worthwhile.

II. EXPERIMENTAL

The measurements were carried out by the conventional radiotracer thin-layer-sectioning technique. However, some of the procedures could not be performed in conventional ways. The high melting temperature [3422 °C (Ref. 46)] and low

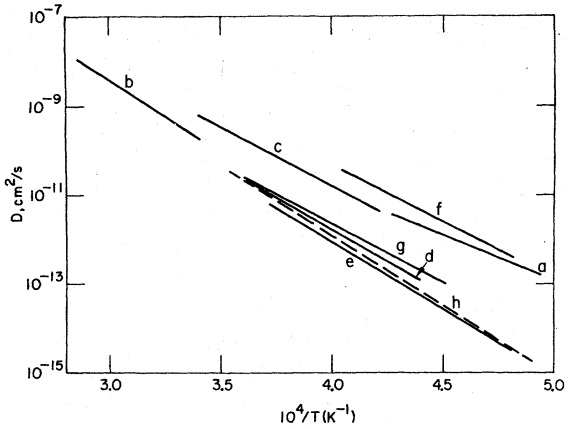

FIG. 1. Arrhenius plots for self-diffusion in tungsten, taken from previous work. The line segments correspond to the temperature range covered in each investigation. References: (a) 37; (b) 36; (c) 35; (d) 38; (e) 39; (f) 40; (g) 41; (h) 42.

sputtering yield of tungsten make deposition of a thin isotope layer by vacuum evaporation or cathodic sputtering difficult. A chemical vapor deposition process was therefore substituted. The annealing temperatures required at the high end of the range (>2600°C) necessitated the use of optical pyrometry with specific calibration techniques. Also, the machining characteristics of tungsten mitigate against sectioning on a lathe. We therefore took thin sections ($\leq$40 nm) by anodizing and stripping, and thicker sections (0.5–2 μm) by grinding.

A. Materials and sample preparation

Single crystals of tungsten, purity 99.999%, 6 or 8 mm in diameter (obtained from Materials Research Corp.), were cut into 3-mm lengths by electrodischarge machining. One face was ground on metallographic paper through size 4/0 paper. Samples to be sectioned by anodizing and stripping were ground further on 6-μm diamond paste, and polished on a vibratory polisher for 48 h with 5-μm Al_2O_3 in ethylene glycol and for 8 h with 0.05-μm Al_2O_3. About 1 μm of material was then removed by anodizing in a 0.4M-KNO_3 + 0.4M-HNO_3 solution at 70 V and stripping in a 5-vol% KOH solution. These samples were sometimes reused for a second run, with only anodizing and stripping as surface preparation.

The γ-emitting ^{187}W ($T_{1/2}$ = 24 h) used as the radiotracer, was laid down by chemical vapor deposition. In principle, this process consists of two steps: WCl_6 powder is irradiated in a reactor and reduced by H_2 at high temperature in the presence of the tungsten samples. The actual manipulation is complicated by the hygroscopicity of WCl_6. Moisture reacts with WCl_6 to form $WOCl_4$, which is not reduced by H_2. (The presence of moisture is easily detected; $WOCl_4$ is red while WCl_6 is dark blue.) The following procedure was therefore developed: A capsule with two necks and a closed end was formed from a quartz tube. The capsule was baked out under a diffusion-pump vacuum, closed off with a valve, and placed into the argon-filled glove box in which the WCl_6 was stored. The valve was removed, a few milligrams of WCl_6 were placed in the capsule and the valve was replaced on the capsule and closed. The capsule was returned to the vacuum system, evacuated, baked out, and sealed at the upper neck under vacuum. After welding into a standard aluminum irradiation can (WCl_6 has a finite vapor pressure at reactor ambient temperatures), the sample was irradiated for ~36 h in a flux of $\sim 5 \times 10^{12}$ n/cm^2 sec. The decanned capsule was put back into the glove box, broken open, and the WCl_6 and the tungsten samples were placed together in a loosely closed tantalum sleeve. This sleeve was sealed into a reduction bomb, which was then removed from the glove box and attached to another vacuum system. The bomb was evacuated and flushed with H_2 several times, backfilled with H_2 to 3.5×10^4 Pa (5-psi positive pressure), heated to ~900 °C for 1 h, and water quenched. After this treatment, the samples could be handled in air. The purity of the radioisotope deposited in this manner was checked by half-life measurement and by high-resolution Ge-Li spectrometry. No radioactive impurities were found. The yield was only a few percent, but enough activity was deposited to obtain adequate counting statistics.

On a few samples, long-lived β-emitting ^{185}W was used as a tracer. This radioisotope, purchased as Na_2WO_4, was deposited dropwise on the sample surface and dried.

B. Annealing

The samples were annealed in an ultrahigh-vacuum electron-beam furnace. The details of the annealing technique have been described by Einziger *et al.*[28] Two crystals were placed in a can with their active faces separated by a tungsten ring. Tantalum cans were used for low-temperature (<2000 °C) anneals, tungsten cans for higher temperatures. One can or two cans, one below the other, were hung from the high-voltage electrode with a tungsten wire.

The temperature was measured with a Leeds and Northrup 8634 disappearing-filament pyrometer. The measurement was always made on a

99.9% blackbody hole so that no emissivity correction had to be made. In the first diffusion anneals, the blackbody hole was the cylindrical space defined by the active faces of the samples and observed through a hole drilled through the side of the can. The D corresponding to this temperature was taken as the geometric mean of the sample D's.[47] As these data were rather scattered, calibration runs were made with matching blackbody holes in the cans and the samples; application of the correction thus obtained substantially decreased the scatter. Subsequently, blackbody holes were spark machined in all samples about 1 mm below the active face, and the sample temperature was measured directly.

As in the work of Einziger *et al.*,[28] the bottom of the sample assembly was hotter than the top, probably owing to a temperature gradient along the electron-emitting filaments. The temperature gradient along the sample assembly, calculated from the values of D obtained from the samples, agreed closely with the gradient measured in a scan of the can surface. Since Einziger *et al.* found that most of the temperature difference was in the gaps between the samples, we believe that no serious error was introduced into our measurements by the temperature gradient within an individual crystal.

The pyrometer and sightglass were calibrated against a tungsten-strip lamp from 1400 to 2500 °C before and after each run. The current-temperature calibration furnished with the lamp was extrapolated from 2300 to 2500 °C. Significant darkening of the sightglass by evaporated tungsten was found only at $T > 2900$ °C, and was reduced by the use of a shutter during the anneal. Preliminary studies showed that the apparent temperature decreased linearly with time as a result of the deposition of tungsten on the sightglass; timing the opening of the shutter with a stopwatch allowed reasonable corrections to be made for tungsten deposition. The pyrometer-sightglass calibrations above 2500 °C were made with a sectored disk,[48] with the assumption that the 2300 °C calibration was correct. Where they overlapped, the different calibration techniques agreed within ±5 °C.

In two high-temperature runs, a Leeds and Northrup 8642 automatic pyrometer was used. The output was recorded on a millivoltmeter, and temperatures were obtained from the recorder chart. Similar corrections were applied.

We have made an extensive analysis of the uncertainty in the temperature. The sources of error considered were: (i) scatter from the fitting procedure used to calculate individual sample temperatures from the calibration studies; (ii) uncertainty in the calibration of the extra high (XH) scale on the model 8634 Leeds and Northrup optical pyrometer above 2600 °C. The uncertainty includes variations in the sectored-disk calibration due to shifts in the effective wavelength with source temperature; (iii) variations in the sightglass correction during individual calibrations; (iv) fluctuations in the tungsten-strip lamp temperatures; (v) observer readings as obtained from a polynomial approximation to the visibility function[48]; (vi) quality of the sample and intersample blackbody holes; (vii) preferential absorption of 0.65-μm light by tungsten or tantalum films deposited during the anneals; and (viii) the steadiness of the power supplies (±2 °C). Based on the above factors, the overall uncertainty in the temperature ranged from ±10 °C at 1400 °C to ±40 °C at 3100 °C.

The length of the anneal was timed with a stopwatch or an electric clock. Annealing times ranged from 5 min to 12 h. Appropriate corrections were made for warmup and for temperature changes. The furnace pressure rose to the 10^{-5}-Pa range during warmup and ranged from 10^{-7} to 10^{-6} Pa during the anneal.

C. Sectioning and counting

1. Anodizing

Anodizing was carried out by the technique proposed by McCargo *et al.*,[49] Pawel and Lundy,[50] and Arkhipova *et al.*[42] The samples to be anodized were masked with tygon paint, and the anodized area was determined from a photograph of the masked crystal. A calibration curve of section thickness versus anodizing voltage for the present study was identical to the curves in the above references. Sections taken under the same conditions were uniformly thick within ±3%; this was determined by sectioning an irradiated crystal and counting the radioactivity in the stripping solutions. The stripping solutions (and anodizing solutions where necessary) were counted in a well-type scintillation counter with a lower-level discriminator. Appropriate corrections were made for background, decay, and dead time. At least 5000 counts over background were recorded for each section. More than 95% of the removed activity was always in the stripping solution; corrections were made for the few percent that leaked into the anodizing solution (this occurred only in the case of the thinnest sections, 3–4 nm).

The actual section thickness was determined from the weight loss of the sample during the entire sectioning process. Weights were determined to ±5 μg on a Mettler M5 balance. Enough sections were taken so that the total weight loss was at least 100 μg. The section thicknesses thus deter-

mined agreed with the calibration curve within a few percent in all but four runs. Blank runs were made by depositing the radioisotope and sectioning the sample without intervening heat treatment.

2. Grinding

A thickness of 0.5 nm was spark-machined off the cylindrical sides of samples to be sectioned by grinding, to eliminate edge efffects. The samples were ground on 400, 600, or 4/0 paper, depending on the desired section thickness. The thickness of the sections was determined by weighing the sample to ±3 μg after removal of each section. The grinding paper and clean-up wipes from each section were placed in a counting bottle and counted as above.

The samples on which β-active ^{185}W had been deposited were also sectioned by grinding. For these samples, the grinding paper plus cleaning materials were counted with a plastic scintillation counter.

III. RESULTS

A. Penetration plots

The direct result of a tracer-diffusion experiment is a plot of activity versus penetration. The solution of the diffusion equation for the thin-layer geometry used in the present study is

$$C = (M/(\pi Dt)^{1/2}) \exp(-X^2/4Dt), \quad (1)$$

where M is the amount of radioisotope deposited on the surface, C is the specific activity of a section whose center is X cm from the surface, D is the diffusion coefficient, and t is the annealing time. The data are therefore plotted on coordinates of log C vs X^2 (Figs. 2 and 3).

The penetration plots from samples sectioned by anodizing were of two types: a straight line followed by a long wiggly tail (Fig 2) or a slightly curved line (Fig. 3, top curve). The tail was observed only for very small penetrations (3-nm sections). We believe the tails are due to surface flaws in the sample, as they appeared on the blanks as well (Fig. 2). The slight curvature in the other plots may be partly due to diffusion along short-circuiting paths and partly due to removal of material from the sides of the depression made by anodizing. Both types of plots were fitted to an equation of the form

$$C = A_1 \exp(-B_1 X^2) + A_2 \exp(-B_2 X^{6/5}) \quad (2)$$

by means of a variable-metric minimization routine.[51] The above functional form is proper for a

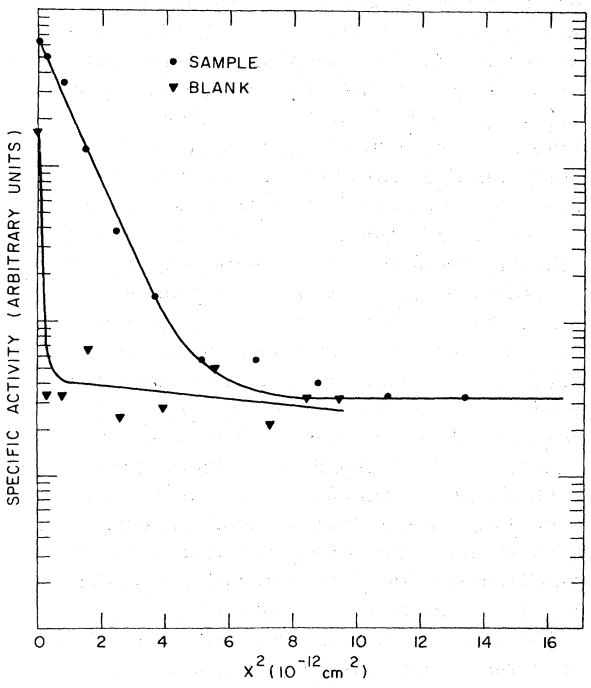

FIG. 2. Penetration plots for self-diffusion in tungsten. "Straight line plus tail" type plots (see text) for a blank run and a sample annealed 4.458×10^4 sec at 1705 K; both sectioned by anodizing.

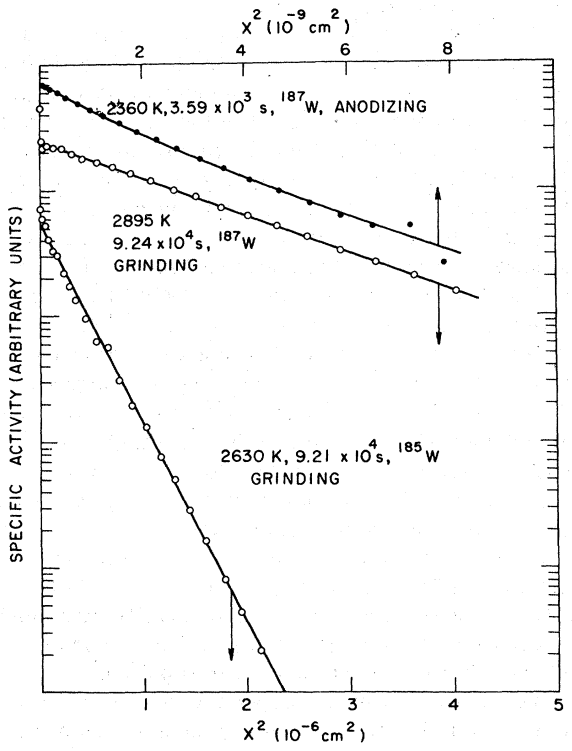

FIG. 3. Penetration plots for self-diffusion in tungsten. Slightly curved plot for sample sectioned by anodizing; straight-line plots for samples sectioned by grinding.

combination of volume and short-circuiting diffusion[52] and fits the "tails" as well, as they are nearly flat; we treat the $X^{6/5}$ term as an artificial correction factor containing no useful information.

Samples sectioned by grinding yielded straight-line penetration plots (Fig. 3). The first few points on penetration plots from samples on which ^{185}W had been dried were high because of holdup of the isotope. Straight-line plots were analyzed by a linearized least-squares fit to Eq. (1).

Five blanks were run. The average "Dt" product $[-4d(\ln C)/dX^2]$ for four of these was $(1.51 \pm 0.60) \times 10^{-14}$ cm^2. (The fifth blank gave a value of 8×10^{-14} cm^2 and was discarded.) This average value was subtracted from the Dt products obtained from the diffusion samples before calculation of D.

B. Diffusion coefficients and their temperature dependence

The diffusion coefficients obtained by the above method are listed in Table I and plotted versus $1/T$ in Fig. 4. The errors corresponding to uncertainty in the temperature were calculated from the factors listed in Sec. IIB. The uncertainty in D was taken as the Pythagorean sum of the uncertainties in the weights, counting rates and annealing time, and from the standard deviation about the least-squares fit to Eq. (1) or (2). At around 1425 °C, the reproducibility of D appeared to be ±50%, and corresponding errors are indicated. At high temperatures, the error in D is small and the scatter is due mostly to uncertainty in the temperature.

The four values of D marked by asterisks in Table I, which were reported in an earlier work,[53] have neither been shown in Fig. 4 nor used in the calculations. The values at 2005 and 2050 °C, which were considerably above the line, could not be reproduced. The values at 2195 and 2338 °C were questionable because the exact temperature calibration was not known.

C. Self-diffusion under electron irradiation

Attempts to measure self-diffusion in tungsten under electron irradiation were unsuccessful. In one run (725 °C, 44 μA/cm^2 of 3-MeV electrons for 6.5 h), the penetration was the same as in the accompanying blank. In the other two runs (1120 and 1200 °C, similar fluxes and times), either radiation damage or chemical contamination during the irradiation changed the anodizing characteristics of the sample to such an extent that sectioning was not possible.

IV. DISCUSSION

A. Temperature dependence of D

The Arrhenius plot of Fig. 4 is curved. This curvature is visible to the naked eye and is confirmed by the systematic deviation of the points from a least-squares fit to a single exponential. Such curvature was not found by Pawel and Lundy[39] or by Arkhipova *et al.*,[42] even though their values of D agree well with ours, because their investigations covered a significantly narrower range of temperatures. The definite curvature in the Arrhenius plot for self-diffusion in tungsten is a major result of our investigation. We have fitted the curved Arrhenius plot of Fig. 4 to the sum of two exponentials by the use of two nonlinear least-squares routines,[54,55] with the result

$$D = 0.04^{0.17}_{0.01} \exp[(-5.4_5 \pm 0.5) eV/kT] + 46^{136}_{16} \exp[(-6.9 \pm 0.6) eV/kT] \text{ cm}^2 \text{ sec}^{-1}, \quad (3)$$

where k is Boltzmann's constant. The values of D were weighted by their variances

$$V = \delta D^2 + \left(\frac{\delta T}{kT^2}\right)^2 \left[Q_1 D_{01} \exp\left(\frac{-Q_1}{kT}\right) + Q_2 D_{02} \exp\left(\frac{-Q_2}{kT}\right)\right]^2, \quad (4)$$

where δD and δT are the uncertainties in the diffusion coefficient and in the temperature, respectively; preliminary estimates of D_{01}, etc., were used. The fit is not skewed, as the deviations are randomly positive (23 points) or negative (24 points). The large standard deviations in the parameters reflect both the experimental scatter (rms deviation of 34%) and the shallowness of the minimum in parameter space; the latter is also confirmed by grid searches with the above programs. The statistical fit of our data to the model of Gilder and Lazarus[18] was equally good.

B. Analysis of the activation enthalpies

1. Phenomenology

Self-diffusion in tungsten is phenomenologically similar to that in the bcc refractory metals Ta, Nb, and V, as shown by the top part of Table II, in which these four elements are ordered in terms of decreasing D at $T = 0.75T_m$. The elements for which diffusion has been measured close to T_m (Nb, V, W, and Cr) all have essentially the same value for $D(T_m)$. Diffusion in Ta has been measured only at temperatures up to $0.76T_m$, so the value of $D(T_m)$ for Ta is not reliable. Also, the narrow temperature range of the diffusion measurements for Ta leads to a large uncertainty in

TABLE I. Self-diffusion in tungsten.

Temperature (K)	Annealing time (sec)	D (cm^2/sec)
1705.0± 9.2	4.458×10^4	$3.17\pm0.25\times10^{-18}$
1716.7± 9.5	1.326×10^5	$9.40\pm3.52\times10^{-18}$
1719.7± 9.6	1.326×10^5	$4.70\pm1.10\times10^{-18}$
1729.0± 8.7	4.463×10^4	$4.89\pm0.63\times10^{-18}$
1767.1± 8.1	4.268×10^4	$1.30\pm0.43\times10^{-17}$
1791.4± 7.8	4.268×10^4	$1.86\pm0.19\times10^{-17}$
1809.6±17.2	1.327×10^5	$3.89\pm0.16\times10^{-17}$
1868.9±11.7	1.333×10^5	$6.70\pm0.15\times10^{-17}$
1870.7± 7.7	1.206×10^4	$7.23\pm0.73\times10^{-17}$
1871.1± 7.8	1.992×10^4	$5.19\pm0.70\times10^{-17}$
1871.9± 8.1	1.198×10^4	$4.16\pm0.58\times10^{-17}$
1874.0± 6.6	1.292×10^4	$1.96\pm0.15\times10^{-16}$
1902.2± 7.5	1.992×10^4	$1.02\pm0.07\times10^{-16}$
1905.5± 6.5	1.292×10^4	$2.82\pm0.14\times10^{-16}$
1905.5±15.7	4.168×10^4	$2.23\pm0.28\times10^{-16}$
1943.6± 7.2	2.164×10^4	$4.30\pm0.35\times10^{-16}$
1970.0± 8.1	4.169×10^4	$5.49\pm0.35\times10^{-16}$
2008.2± 7.7	2.164×10^4	$1.32\pm0.07\times10^{-15}$
2015.2±15.4	1.124×10^4	$1.09\pm0.18\times10^{-15}$
2056.4± 8.5	1.001×10^4	$2.90\pm0.30\times10^{-15}$
2078.9± 8.6	1.127×10^4	$2.70\pm0.16\times10^{-15}$
2127.5± 9.1	3.72×10^3	$7.13\pm0.52\times10^{-15}$
2131.2± 9.3	3.72×10^3	$8.68\pm0.62\times10^{-15}$
2202.7±11.2	3.61×10^3	$1.85\pm0.10\times10^{-14}$
2232.7±11.4	3.61×10^3	$3.27\pm0.07\times10^{-14}$
2255.6±10.7	3.71×10^3	$1.88\pm0.05\times10^{-13}$ [a]
2315.2± 7.1	3.59×10^3	$8.78\pm0.26\times10^{-14}$
2327.3±11.8	3.71×10^3	$4.51\pm0.28\times10^{-13}$ [a]
2334.8±10.6	6.45×10^2	$9.62\pm0.26\times10^{-14}$
2352.3±10.9	6.52×10^2	$1.34\pm0.06\times10^{-13}$
2360.2± 7.2	3.59×10^3	$1.42\pm0.05\times10^{-13}$
2480.2±14.6	4.27×10^4	$2.03\pm0.03\times10^{-12}$ [a]
2630.2±16.5	4.27×10^4	$2.39\pm0.03\times10^{-12}$ [a]
2630.2±11.7	9.21×10^3	$7.22\pm0.23\times10^{-12}$
2650.6±13.2	9.90×10^3	$5.82\pm0.23\times10^{-12}$
2739.3±11.9	9.22×10^3	$2.00\pm0.08\times10^{-11}$
2759.6±13.6	9.90×10^3	$1.28\pm0.02\times10^{-11}$
2855.4±20.7	9.91×10^3	$3.69\pm0.04\times10^{-11}$
2869.4±21.3	9.91×10^3	$4.31\pm0.10\times10^{-11}$
2895.2±11.3	9.24×10^3	$3.99\pm0.01\times10^{-11}$
2911.2±12.1	9.24×10^3	$3.00\pm0.09\times10^{-11}$
2998.0±14.0	1.49×10^3	$1.15\pm0.02\times10^{-10}$
3080.7±24.1	1.00×10^3	$3.11\pm0.06\times10^{-10}$
3099.1±15.0	1.51×10^3	$2.51\pm0.04\times10^{-10}$
3199.8±15.6	1.00×10^3	$6.32\pm0.08\times10^{-10}$
3242.3±31.8	6.86×10^2	$1.21\pm0.03\times10^{-9}$
3243.3±26.5	5.04×10^2	$1.45\pm0.10\times10^{-9}$
3309.4±24.0	6.94×10^2	$1.80\pm0.03\times10^{-9}$
3319.0±43.5	4.77×10^2	$1.96\pm0.02\times10^{-9}$
3342.7±27.2	5.04×10^2	$2.42\pm0.04\times10^{-9}$
3408.9±33.1	4.75×10^2	$3.08\pm0.04\times10^{-9}$

[a] See text.

the parameters. A pattern is nevertheless evident in the diffusion data of Table II. The ratio of the activation energies is the same for each element within a few percent, but the uncertainty in each ratio is ±15%. The absolute values of the parameters increase as the diffusion coefficient of the element decreases.

The data for chromium[34] and the recent data for

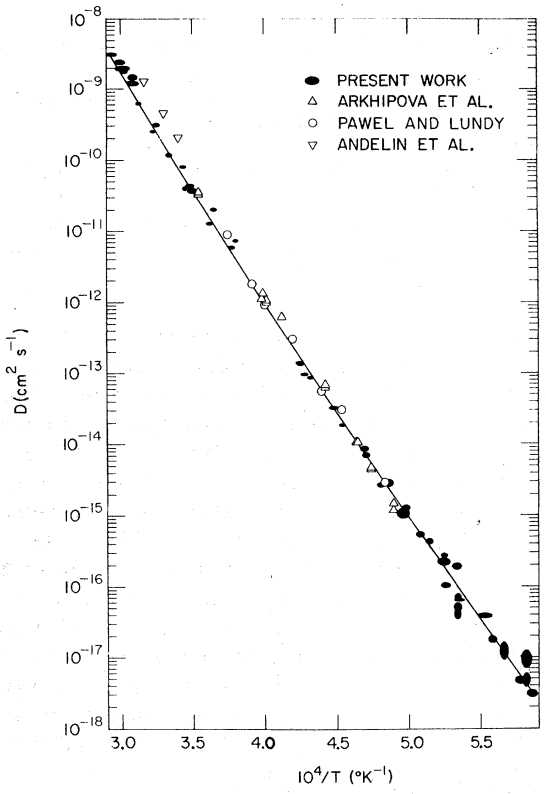

FIG. 4. Arrhenius plot for self-diffusion in tungsten. Data from present investigation and from Refs. 36, 39, and 42. The ellipses on our points represent the calculated uncertainties in D (vertical axis) and $1/T$ (horizontal axis).

molybdenum[33] were obtained over a narrower temperature range (Cr from $0.64T_m$ to $0.98T_m$, Mo from $0.47T_m$ to $0.74T_m$) and were originally fitted to single exponentials. Let us assume, nevertheless, that diffusion in Cr and Mo conforms to the pattern set by Ta, Nb, V, and W, i.e., that the data fit a sum of two exponentials with $Q_2/Q_1 = 1.28$, $D_2(T_m)/D_1(T_m) = 11$, and $D(T_m) = 1.9 \times 10^{-8}$ cm^2 sec^{-1} (the averages of the values for Ta, Nb, V, and W). If we then estimate Q_1/T_m for Cr and Mo from the trend indicated by the other four metals, we obtain the other parameters shown in the bottom two lines of Table II. The values of D obtained from these parameters agree very well with the experimental values for both Mo and Cr. The curvature expected in the Arrhenius plots determined from the parameters given in Table II is not seen in the experimental data for Cr and Mo because of the narrow temperature ranges and the errors in the individual values of D. For this reason, it would be of interest to extend the temperature range of the diffusion measurements in Cr and Mo and further check the pattern that is apparent in Table II.

A similar pattern can be seen in Table III, where the fcc metals are arranged in order of decreasing diffusion coefficient for a temperature of $0.75T_m$. The activation energies increase with decreasing D for both the high- and low-temperature processes, but the Q_2/Q_1 are similar to those found for bcc transition metals, again with an uncertainty of ±15% in the individual ratios. The strong evidence for the single-vacancy–divacancy mechanism in the fcc metals[16,17] and the similarity of Tables II and III suggest that diffusion in the bcc refractory metals also takes place by a single-vacancy–divacancy mechanism, as proposed earlier.[57,58]

2. *Relation of the diffusion enthalpies to defect parameters*

The "low-temperature" diffusion process in W can be identified as diffusion by single vacancies, according to the following argument. The apparent enthalpy of formation of single vacancies, obtained from quenching measurements,[43,44,59] is $(H_{1v}^f)_{\text{eff}}$

TABLE II. Diffusion parameters for bcc refractory metals.

Element	D_{01} (cm^2 sec^{-1})	Q_1/T_m cal K^{-1}	D_{02} (cm^2 sec^{-1})	Q_2/T_m cal K^{-1}	Q_2/Q_1	$D_2(T_m)/D_1(T_m)$	$D(T_m)$ (cm^2 sec^{-1})	Reference
Ta[a]	1.8×10^{-2}	28.7	10.0	37.7	1.32	6	6.6×10^{-8}	29
Nb	8.0×10^{-3}	30.5	3.7	38.2	1.25	10	1.8×10^{-8}	28
V[a]	1.4×10^{-2}	31.2	7.5	39.8	1.27	7	1.7×10^{-8}	27
W	4.0×10^{-2}	34.0	46.0	43.0	1.27	13	1.9×10^{-8}	Present work
Mo[b]	1.0×10^{-1}	36.0	200.0	46.0	1.28	11	1.9×10^{-8}	33
Cr[b]	8.8×10^{-1}	40.0	2720.0	51.2	1.28	11	1.9×10^{-8}	34

[a] Parameters calculated from the data of Refs. 29 and 27 by the program of Ref. 54.
[b] See text for the method of calculation of these parameters.

TABLE III. Diffusion parameters for fcc metals.

Element	D_{01} ($cm^2\,sec^{-1}$)	Q_1/T_m cal K^{-1}	D_{02} ($cm^2\,sec^{-1}$)	Q_2/T_m cal K^{-1}	Q_2/Q_1	$D_2(T_m)/D_1(T_m)$	$D(T_m)$ ($cm^2\,sec^{-1}$)	Reference
Au	0.07	30.9	0.05	39.0	1.26	0.09	1.3×10^{-8}	56
Ag	0.04	32.9	4.8	40.9	1.24	2.10	8.0×10^{-9}	17
Cu	0.16	35.2	6.4	44.0	1.25	0.47	4.7×10^{-9}	17
Ni	0.92	38.5	37.0	49.4	1.28	0.17	4.1×10^{-9}	17

$= 3.6 \pm 0.2$ eV; the apparent enthalpy of motion of single vacancies, obtained from measurements of the annealing of quenched-in resistivity,[44,59] is $(H_{1v}^m)_{eff} = 1.8 \pm 0.1$ eV. The observation of voids by electron microscopy[44] indicates that these measurements indeed relate to vacancy formation and motion. The reliability of these single-vacancy parameters has been extensively discussed in a recent conference.[19,20] Since the sum of the measured H_{1v}^f and H_{1v}^m just equals Q_1, it is reasonable to assume that the low-temperature diffusion process is the result of the motion of single vacancies.

The entropy of activation for diffusion ΔS can be obtained from the equation

$$D_0 = \gamma a_0^2 \nu f \exp(\Delta S/k), \tag{5}$$

where γ is a geometrical constant that depends on the cell geometry and the assumed jump mechanism, ν is an average atomic-vibration frequency, a_0 is the lattice parameter, and f is the correlation factor. If the low-temperature process is the single-vacancy mechanism, then $\gamma = 1$, $f = 0.727$, and ν can be determined[16] from

$$\nu_{1v} = (1/a)(2H_{1v}^m/3M)^{1/2}, \tag{6}$$

where M is the atomic mass. The activation entropy for diffusion determined from the present data and Eq. (5) is $3k$. The formation entropy for a single vacancy, determined from quenching experiments,[59] is $2k$. The activation entropies determined for the other bcc refractory metals on the basis of the same assumptions are $1.2k$ for V, $0.9k$ for Nb, and $1.6k$ for Ta. Thus the entropies found for the low-temperature process in the group-V bcc metals are similar to those found for fcc metals.[17,19,60] The entropy for diffusion in W is higher and the values determined from the estimated fits for Mo and Cr are even larger at $4k$ and $6k$, respectively. This suggests a strongly relaxed vacancy[17] in W, Mo, and Cr; such relaxation would lead to smaller isotope effects, as observed in Cr self-diffusion.[34]

The high-temperature mechanism is the dominant diffusion process above 2375 K and accounts for 93% of the diffusion at the melting point. The defect responsible for the high-temperature mechanism is, however, not easy to identify. A low-mobility defect in high concentration is unlikely, as such a defect would then be the dominant defect observed in quenched tungsten [$T_0 > 2500$ K (Ref. 59)]; this is contrary to the results of the quenching experiments, which indicate that monovacancies are retained. On the other hand, a high-mobility defect in low concentration could still allow single vacancies to be the dominant defect observed in quenched tungsten. Such a high-mobility defect could be a divacancy, as has been suggested in the previous section, or an interstitial as recently proposed for the high-temperature diffusion mechanism in copper.[61] The large values of the formation entropy for interstitials would fit with the rather large preexponential factors (D_{02}) found for the bcc transition metals (Table II).

The model of Gilder and Lazarus[18] with its temperature-dependent energies leads to an inconsistency. The model leads one to expect that the defect-formation energy obtained by quenching samples from $T > 2500$ K would correspond to the high-temperature value of H_{1v}^f, and that the defect-motion energy obtained from annealing studies at $T < 1200$ K would correspond to the low-temperature value of H_{1v}^m. If $H^f = 2H^m$ independent of temperature,[44,59] then $H^f(2500\text{ K}) + H^m(1200\text{ K}) = 6.0$ eV, which is different from the observed 5.4_5 eV. While the Gilder and Lazarus model fits the diffusion data as well as does a two defect model, it is not nearly as consistent with other experimental results on point defects.[62]

V. CONCLUSIONS

We can draw the following conclusions: (i) The diffusion behavior of tungsten is phenomenologically similar to that of the group V-B metals. (ii) The Arrhenius plot for self-diffusion in tungsten is curved, and can be fitted to a sum of two exponen-

tials with activation energies of $5.4_5 \pm 0.5$ and 6.9 ± 0.6 eV. (iii) The lower of these activation energies corresponds to diffusion by single vacancies. The higher activation energy can represent motion either by divacancies or by interstitials.

Note added in proof. The measurements of Ref. 33 have been extended over a wide range of temperatures. Non-Arrhenius behavior was found and the parameters agree well with the estimates given in Table II. [K. Maier, G. Rein, and H. Mehrer, Z. Metallkd. (to be published).]

ACKNOWLEDGMENTS

We thank W. Cann for spark machining of samples, R. J. Thorn and his group for help with optical pyrometry, R. W. Siegel for his constant encouragement and helpful comments, N. L. Peterson and K. Maier for permission to quote unpublished work, and Jean Jordan for helping to develop the chemical vapor deposition technique. This research was supported by the U. S. Department of Energy.

[1]S. J. Rothman, N. L. Peterson, and J. T. Robinson, Phys. Status Solidi 39, 635 (1970).
[2]P. Reimers and D. Bartdorff, Phys. Status Solidi B 50, 305 (1972).
[3]N. Q. Lam, S. J. Rothman, H. Mehrer, and L. J. Nowicki, Phys. Status Solidi B 57, 225 (1973).
[4]J. G. E. M. Backus, H. Bakker, and H. Mehrer, Phys. Status Solidi B 64, 151 (1974).
[5]S. J. Rothman and N. L. Peterson, Phys. Status Solidi 35, 305 (1969).
[6]D. Bartdorff, dissertation (Technical University of Berlin, 1972) (unpublished).
[7]K. Maier, Phys. Status Solidi A 44, 567 (1977).
[8]N. Q. Lam, S. J. Rothman, and L. J. Nowicki, Phys. Status Solidi 63, K29 (1974).
[9]S. M. Makin, A. H. Rowe, and A. D. LeClaire, Proc. Phys. Soc. Lond. 70, 545 (1957).
[10]H. M. Gilder and D. Lazarus, J. Phys. Chem. Solids 26, 2081 (1965).
[11]A. Gainotti and L. Zecchina, Nuovo Cimento B 40, 295 (1965).
[12]W. Rupp, U. Ermert, and R. Sizmann, Phys. Status Solidi 33, 509 (1969).
[13]C. Herzig, H. Eckseler, W. Bussman and D. Cardis, in *Properties of Atomic Defects in Metals*, edited by N. L. Peterson and R. W. Siegel (North-Holland, Amsterdam, 1978), p. 61; J. Nucl. Mater. 69—70, 61 (1978).
[14]H. Bakker, Phys. Status Solidi 28, 569 (1968).
[15]K. Maier, H. Mehrer, E. Lessmann and W. Schüle, Phys. Status Solidi B 78, 689 (1976).
[16]A. Seeger and H. Mehrer, in *Vacancies and Interstitials in Metals*, edited by A. Seeger, D. Schumacher, W. Schilling, and J. Diehl (North-Holland, Amsterdam, 1970), p. 1.
[17]N. L. Peterson, J. Nucl. Mater. 69-70, 3 (1978).
[18]H. M. Gilder and D. Lazarus, Phys. Rev. B 11, 4916 (1975).
[19]R. W. Siegel, J. Nucl. Mater. 69-70, 117 (1978).
[20]R. W. Balluffi, J. Nucl. Mater. 69-70, 240 (1978).
[21]For a review, see Ref. 17 or N. L. Peterson, Comments Solid State Phys. 8, 93 (1978).
[22]J. F. Murdock, T. S. Lundy, and E. E. Stansbury, Acta Metall. 12, 1033 (1964).
[23]J. I. Federer and T. S. Lundy, Trans. Metall. Soc. AIME 227, 592 (1963).
[24]*Diffusion in Body-Centered Cubic Metals* (American Society for Metals, Cleveland, 1965).
[25]T. S. Lundy and C. J. McHargue, Trans. Metall. Soc. AIME 233, 243 (1965).
[26]R. F. Peart, J. Phys. Chem. Solids 26, 1853 (1965).
[27]J. Pelleg, Philos. Mag. 29, 383 (1974).
[28]R. E. Einziger, J. N. Mundy, and H. A. Hoff, Phys. Rev. B 17, 440 (1978).
[29]R. E. Pawel and T. S. Lundy, J. Phys. Chem. Solids 26, 937 (1965).
[30]J. N. Mundy, Phys. Rev. B 3, 2431 (1971).
[31]J. N. Mundy, T. E. Miller, and R. J. Porte, Phys. Rev. B 3, 2445 (1971).
[32]J. Askill and D. H. Tomlin, Philos. Mag. 8, 997 (1963).
[33]K. Maier, G. Rein, and H. Mehrer (private communication).
[34]J.N. Mundy, C. W. Tse, and W. D. McFall, Phys. Rev. B 13, 2349 (1976).
[35]W. Danneberg, Metall (Berlin) 15, 977 (1961).
[36]R. L. Andelin, J. D. Knight, and M. Kahn, Trans. Metall. Soc. AIME 233, 19 (1965).
[37]G. M. Neumann and W. Hirschwald, Z. Naturforsch. A 21, 812 (1966).
[38]L. N. Laricov, L. F. Chernaya, and T. K. Yatsenko, *Properties and Applications of Heat-Resisting Alloys* (Nauka, Moscow, 1966), p. 28.
[39]R. E. Pawel and T. S. Lundy, Acta Metall. 17, 979 (1969).
[40]G. B. Fedorov, F. I. Zhomov, and E. A. Smirnov, in *Metallurgy and Metallography of Pure Metals*, edited by V. S. Yemelyanov and A. I. Yevstyukhin (Atomizdat, Moscow, 1969), Vol. 8, p. 145.
[41]A. A. Korolyev, L. V. Pavlinov, and M. I. Gavrilyuk, Fiz. Met. Metalloved. 33, 295 (1972).
[42]N. K. Arkhipova, S. M. Klotsman, Y. A. Rabovskii, and A. N. Timofeyev, Fiz. Met. Metalloved. 43, 779 (1977).
[43]W. Kunz, Phys. Status Solidi B 48, 387 (1971).
[44]K.-D. Rasch, R. W. Siegel, and H. Schultz, J. Nucl. Mater. 69-70, 622 (1978).
[45]K. Maier, H. Metz, D. Herlach, and H. E. Schaeffer, J. Nucl. Mater. 69-70, 589 (1978).
[46]A. Cezairliyan, High Temp. Sci. 4, 248 (1972).
[47]R. E. Einziger and J. N. Mundy, Rev. Sci. Instrum. 47, 1547 (1976).
[48]H. J. Kostkowski and R. D. Lee, *Theory and Methods of Optical Pyrometry*, NBS Monograph No. 41 (U.S. GPO, Washington, 1962).
[49]M. McCargo, J. A. Davies, and F. Brown, Can. J. Phys. 41, 1231 (1963).
[50]R. E. Pawel and T. S. Lundy, J. Electrochem. Soc. 115, 233 (1968).
[51]M. Gabriel, Special-Purpose Language for Least-Squares Fits, Argonne National Laboratory Report No. ANL-7495, 1968 (unpublished).
[52]T. Suzuoka, Trans. Jpn. Inst. Met. 2, 25 (1961).

[53]J. N. Mundy, S. J. Rothman, N. Q. Lam, H. A. Hoff, and L. J. Nowicki, J. Nucl. Mater. 69-70, 526 (1978).
[54]T. Antaya (unpublished).
[55]A. J. Barr, J. H. Goodnight, J. P. Sall, and J. T. Helwig, *A User's Guide to SAS* (Statistical Analysis System Institute, Raleigh, N.C., 1976), p.193.
[56]R.P. Sahu, K. C. Jain, and R. W. Siegel, J. Nucl. Mater. 69-70, 264 (1978).
[57]R. F. Peart and J. Askill, Phys. Status Solidi 23, 263 (1967).
[58]H. Mehrer, P. Kunz, and A. Seeger, in *Defects in Refractory Metals* (SCK/CEN, Mol, Belgium 1972), pp. 183-191.
[59]K.-D. Rasch, H. Schultz, and R. W. Siegel, Philos. Mag. A 37, 567 (1978).
[60]A. Seeger, Cryst. Lattice Defects 4, 221 (1973).
[61]W. Schilling, J. Nucl. Mater. 69-70, 465 (1978).
[62]N. L. Peterson, Comments Solid State Phys. 8, 107 (1978).